

## Supporting Information

### Disentangling chemical pressure and superexchange effects in lanthanide-organic valence tautomerism

Anton Viborg,<sup>†</sup> Maja A. Dunstan,<sup>†\*</sup> Nathan J. Yutronkie,<sup>‡</sup> Amit Chanda,<sup>||</sup> Felix Trier,<sup>||</sup> Nini Pryds,<sup>||</sup>  
Fabrice Wilhelm,<sup>‡</sup> Andrei Rogalev,<sup>‡</sup> Dawid Pinkowicz,<sup>§</sup> Kasper S. Pedersen<sup>†\*</sup>

<sup>†</sup>Department of Chemistry, Technical University of Denmark, DK-2800 Kgs. Lyngby Denmark

<sup>‡</sup>European Synchrotron Radiation Facility, 38000 Grenoble, France.

<sup>§</sup>Faculty of Chemistry, Jagiellonian University, 30-387 Kraków, Poland.

<sup>||</sup>Department of Energy Conversion and Storage, Technical University of Denmark, DK-2800 Kgs. Lyngby,  
Denmark

*Chemical Science*

## Materials and Methods

### Synthetic Procedures

All manipulations were performed in an Ar-filled glovebox (Inert I-Lab, O<sub>2</sub> < 0.1 ppm, H<sub>2</sub>O < 0.5 ppm) unless otherwise stated. The reagents 1,2-dimethoxyethane (dme; 99.5%, Sigma-Aldrich), SmI<sub>2</sub> (>99.99%, Thermo Fisher Scientific), CaI<sub>2</sub> (99.95%, Sigma-Aldrich), SrI<sub>2</sub> (99.99%, Thermo Fisher Scientific), pyrazine (pyz; >99%, Sigma-Aldrich) were obtained from commercial suppliers and used as received. Tetrahydrofuran (thf) and diethyl ether were obtained from an Inert solvent purification system and stored over molecular sieves. The syntheses of SmI<sub>2</sub>(pyz)<sub>2</sub>(thf), SmBr<sub>2</sub>(pyz)<sub>2</sub>(thf), SrI<sub>2</sub>(pyz)<sub>2</sub>(thf), CaI<sub>2</sub>(pyz)<sub>2</sub>(thf), and all solid solutions thereof were carried out via a modified procedure from Dunstan et al.<sup>1</sup> All samples were stored at -20 °C under Ar.

**SmBr<sub>2</sub>(thf)<sub>2</sub>:** The compound was synthesized according to a modified procedure by Szostak et al.<sup>2</sup> A blue solution of SmI<sub>2</sub> (220 mg, 0.54 mmol) in thf (2 mL) was added to a colorless solution of LiBr (220 mg, 2.53 mmol) in thf (1 mL). The resulting bright purple solution was stirred for 15 minutes. The solution was left at -20 °C overnight before filtration. The precipitate was washed twice with cold Et<sub>2</sub>O (ca. 0.5 mL). The dark purple precipitate was stored at -20 °C under inert conditions as it readily decomposes slowly at ambient temperature. Yield: 200 mg (0.44 mmol, 81%)

**SmI<sub>2</sub>(pyz)<sub>2</sub>(thf) (0%):** A warm solution (~60 °C) of SmI<sub>2</sub> (100 mg, 0.25 mmol) in thf (2.5 mL) was added dropwise to a melt of pyrazine (800 mg, 10 mmol). A dark blue precipitate formed immediately, and the mixture was allowed to cool to room temperature. The dark blue-grey solid was then isolated by vacuum filtration, washed with diethyl ether (2 × 0.5 mL), and dried. Yield: 100 mg (0.16 mmol, 63%). Anal. calcd. (found) for SmI<sub>2</sub>(pyz)<sub>2</sub>(thf): C, 22.65% (22.33%), H, 2.53% (2.50%), N, 8.80% (8.69%).

**SmBr<sub>2</sub>(pyz)<sub>2</sub>(thf) (100%):** The compound was synthesized analogously to SmI<sub>2</sub>(pyz)<sub>2</sub>(thf) using SmBr<sub>2</sub>(thf)<sub>2</sub> and a 1/1 v/v mixture of thf and dme as the reaction solvent. Amounts used: SmBr<sub>2</sub>(thf)<sub>2</sub> (64.1 mg, 0.141 mmol), pyrazine (674 mg, 8.41 mmol), dme (1.5 mL), thf (1.5 mL). Yield: 72 mg (0.13 mmol, 94%). Anal. calcd. for SmBr<sub>2</sub>(pyz)<sub>2</sub>(thf): C, 26.57% (26.20%), H, 2.97% (2.95%), N, 10.33% (10.28%).

**10% and 20%:** The solid solutions of SmBr<sub>2</sub>(pyz)<sub>2</sub>(thf) in SmI<sub>2</sub>(pyz)<sub>2</sub>(thf) were synthesized by dissolving appropriate amounts of SmI<sub>2</sub> and SmBr<sub>2</sub>(thf)<sub>2</sub> in thf/dme 1:1 (3 mL) and adding the dark-blue solution dropwise to a melt of pyrazine. The resultant precipitate was isolated in the same manner as **0%** and **100%**.

**10%:** Amounts used:  $\text{SmBr}_2(\text{thf})_2$  (13 mg, 28  $\mu\text{mol}$ );  $\text{SmI}_2$  (99 mg, 0.25 mmol); pyrazine (1.0 g, 13 mmol). Yield: 126 mg (0.20 mmol, 73%). Anal. calcd. (found) for  $\text{SmBr}_{0.2} \text{I}_{1.8}(\text{pyz})_2(\text{thf})$ : C, 22.99% (23.02%), H, 2.57% (2.55%), N, 8.94% (8.95%), Br, 2.55% (2.90%), I, 36.43% (35.88%).

**20%:** Amounts used:  $\text{SmBr}_2(\text{thf})_2$  (24 mg, 53  $\mu\text{mol}$ );  $\text{SmI}_2$  (86 mg, 0.21 mmol); pyrazine (1.0 g, 13 mmol). Yield: 135 mg (0.22 mmol, 82%). Anal. calcd. (found) for  $\text{SmBr}_{0.4} \text{I}_{1.6}(\text{pyz})_2(\text{thf})$ : C, 23.34% (22.89%), H, 2.61% (2.58%), N, 9.07% (8.93%), Br, 5.17% (5.05%), I, 32.87% (32.25%).

**Ca-10%, Ca-20% and Ca-100%:** The solid solutions of  $\text{CaI}_2(\text{pyz})_2(\text{thf})$  in  $\text{SmI}_2(\text{pyz})_2(\text{thf})$  were made analogously to the other solid solutions, using thf as the solvent.

**Ca-10%:** Amounts used:  $\text{CaI}_2$  (7.5 mg, 26  $\mu\text{mol}$ );  $\text{SmI}_2$  (90 mg, 0.22 mmol); pyrazine (800 mg, 10 mmol); thf (2 mL). Yield: 109 mg (0.17 mmol, 70%). Anal. calcd. (found) for  $\text{Sm}_{0.9} \text{Ca}_{0.1} \text{I}_2(\text{pyz})_2(\text{thf})$ : C, 23.05% (22.92), H, 2.58% (2.55%), N, 8.96% (8.95%), Ca, 0.64% (0.66%).

**Ca-20%:** Amounts used:  $\text{CaI}_2$  (15 mg, 50  $\mu\text{mol}$ );  $\text{SmI}_2$  (80 mg, 0.20 mmol); pyrazine (800 mg, 10 mmol); thf (2 mL). Yield: 129 mg (210  $\mu\text{mol}$ , 85%). Anal. calcd. (found) for  $\text{Sm}_{0.8} \text{Ca}_{0.2} \text{I}_2(\text{pyz})_2(\text{thf})$ : C, 23.46% (23.18%), H, 2.63% (2.59), N, 9.12% (9.04%), Ca, 1.30% (1.33%).

**Ca-100%:** Amounts used:  $\text{CaI}_2$  (29 mg, 100  $\mu\text{mol}$ ); pyrazine (480 mg, 6.0 mmol), thf (1.5 mL). Yield: 40 mg (76  $\mu\text{mol}$ , 76%).

**Sr-7.5%, Sr-15% and Sr-100%:** The solid solutions of  $\text{SrI}_2(\text{pyz})_2(\text{thf})$  in  $\text{SmI}_2(\text{pyz})_2(\text{thf})$  were made analogously to the other solid solutions using thf as the solvent.

**Sr-7.5%:** Amounts used:  $\text{SrI}_2$  (8.6 mg, 25  $\mu\text{mol}$ );  $\text{SmI}_2$  (91 mg, 0.23 mmol); pyrazine (800 mg, 10 mmol); thf (2 mL). Yield: 99 mg (0.16 mmol, 63%). Anal. calcd. (found) for  $\text{Sm}_{0.925} \text{Sr}_{0.075} \text{I}_2(\text{pyz})_2(\text{thf})$ : C, 22.81% (22.53%), H, 2.55% (2.54%), N, 8.87% (9.03%), Sr, 1.04% (1.06%).

**Sr-20%:** Amounts used:  $\text{SrI}_2$  (15 mg, 44  $\mu\text{mol}$ );  $\text{SmI}_2$  (80 mg, 0.20 mmol); pyrazine (800 mg, 10 mmol); thf (2 mL). Yield: 104 mg (0.17 mmol, 69%). Anal. calcd. (found) for  $\text{Sm}_{0.85} \text{Sr}_{0.15} \text{I}_2(\text{pyz})_2(\text{thf})$ : C, 22.99% (22.96%), H, 2.57% (2.61%), N, 8.94% (9.12%), Sr, 2.10% (1.96%).

**Sr-100%:**  $\text{SrI}_2$  (23 mg, 67  $\mu\text{mol}$ ); pyrazine (200 mg, 2.5 mmol); thf (1.25 mL). Yield: 25 mg (43  $\mu\text{mol}$ , 64%).

## X-ray Crystallography

Single crystals of  $\text{SmI}_2(\text{pyz})_2(\text{thf})$  (**0%**),  $\text{CaI}_2(\text{pyz})_2(\text{thf})$  (**Ca-100%**), and  $\text{SrI}_2(\text{pyz})_2(\text{thf})$  (**Sr-100%**) were covered in polybutene oil (>90%, Sigma-Aldrich) under an Ar atmosphere, mounted on a nylon loop and immediately subjected to an  $\text{N}_2$  stream. Single crystal diffraction data were obtained on a SuperNova Dual Source CCD-diffractometer using a  $\text{Cu K}\alpha$  source. Data for **0%** were collected at 170 K, 230 K, and 295 K, while data for **Ca-100%** and **Sr-100%** were collected at 295 K. All data were reduced in CrysAlisPro<sup>3</sup> and corrected using a numerical absorption correction based on Gaussian integration over a multi-faceted crystal model. All structures were solved with the SHELXS<sup>4</sup> structure solution program using direct methods and refined with the SHELXL<sup>5</sup> refinement package using least squares minimization on all data, in the Olex2 software.<sup>6</sup> All non-hydrogen atoms were refined anisotropically, and hydrogen atoms were placed at geometrical estimates and refined using a riding model. The pendant thf ligand is disordered over a plane of symmetry and was refined with rigid bond restraints and similar thermal displacement parameters for neighboring atoms.

All powder X-ray diffraction (PXRD) data were collected using  $\text{Cu K}\alpha$  radiation ( $\lambda = 1.5406 \text{ \AA}$ ) in flame-sealed borosilicate glass capillaries ( $\varnothing$  0.5 mm, wall thickness 0.01 mm) filled under an Ar atmosphere. Measurements were performed on a Malvern Panalytical Empyrean powder X-ray diffractometer equipped with a 1Der detector. Rietveld refinements were performed in the HighScore Plus 5.1.0 program suite.<sup>7</sup> The structures of **0%**, **10%**, **20%**, **Ca-10%**, **Ca-20%**, **Sr-7.5%**, and **Sr-15%** solid solutions were refined against the 230 K single crystal structure of  $\text{SmI}_2(\text{pyz})_2(\text{thf})$  (**HT-0%**). The  $\text{SmBr}_2(\text{pyz})_2(\text{thf})$  (**100%**) structure was refined against the 170 K single crystal structure of  $\text{SmI}_2(\text{pyz})_2(\text{thf})$  (**LT-0%**). Peak profiles were fit with a pseudo-Voigt peak function and the atomic positions of Sm, Ca, Sr, I, Br, N, O, and C were refined with the relative occupancies of I/Br, Sm/Ca, and Sm/Sr fixed to the experimentally determined elemental ratios. For each refinement, a background function was defined and subtracted from the data to remove amorphous scattering from the capillary. Variable-temperature PXRD data were acquired on  $\text{SmBr}_2(\text{pyz})_2(\text{thf})$  (**100%**) on a SuperNova Dual Source CCD-diffractometer.

## Magnetization

Magnetization data for all samples were collected on a QuantumDesign Dynacool Physical Properties Measurement System (PPMS) with the vibrating sample magnetometer (VSM) option. Temperature sweeps were performed in an applied magnetic field of 1 T, between 3 K and 270 K with a sweep rate of  $0.5 \text{ K min}^{-1}$ . Magnetization vs field measurements for **10%** and **20%** were obtained at temperatures between 3 K and 20 K in applied magnetic fields between 0 T and 9 T. Polycrystalline samples (10–20 mg) were loaded into standard QuantumDesign PTFE powder

capsules under an Ar atmosphere, wrapped in PTFE tape, and quickly inserted into the PPMS chamber. The data were corrected for intrinsic diamagnetism of the samples.

### **X-ray Absorption Spectroscopy**

X-ray absorption spectroscopy experiments at the Sm  $L_2$ -edge were performed at the ID12 beamline at the European Synchrotron Radiation Facility (ESRF, France). The samples were prepared as polycrystalline powders in flame-sealed borosilicate glass capillaries ( $\varnothing$  2.0 mm, wall thickness of 0.01 mm). The data were collected at  $\sim$ 50 K and room temperature, using total fluorescence yield detection mode, and were not corrected for re-absorption effects. The intensity of the incident X-ray beam was carefully attenuated to avoid radiation damage of the sample. All spectra were normalized in the same manner to allow for comparison.

### **Electrical Conductivity**

The samples were prepared as polycrystalline powders and pressed between two stainless steel screws in a PTFE cell ( $\varnothing$  0.33 cm) to a thickness of 0.4–0.7 mm. The cell was mounted on a dc resistivity puck (QuantumDesign) with thermal varnish. Each screw was wrapped with Cu wire soldered to the terminals of the puck. The puck was mounted in a QuantumDesign PPMS and connected to a Keithley 6487 picoammeter via a custom Aivon BoBoX breakout box. The measurements were controlled via a homebuilt code written in the LabView software. Variable-temperature resistivity was measured with sweep-rates of 1–2 K min<sup>-1</sup>. The excitation voltage used for all measurements was 10 V with a current limit of 25 mA, and 10–30 measurements were averaged for each data point.

### **Differential Scanning Calorimetry**

Differential scanning calorimetry was measured in a Netzsch DSC214 Polyma instrument in TA Instruments Tzero aluminum pans with hermetic lids. The compounds were measured in the range 298–100 K with sweep rates of 1 K min<sup>-1</sup> and 2 K min<sup>-1</sup>. The reference pan was an empty Tzero pan with a hermetic lid sealed under an Ar atmosphere. The pans were filled with 5–12 mg of compound carefully sealed under Ar by crimping with hermetic lids.

### **Elemental Analysis**

Elemental analysis was performed by Mikroanalytisches Laboratorium Kolbe (Fraunhofer Institut Umsicht, Oberhausen, Germany).

## Supplementary Data

### Single Crystal and Powder X-Ray Diffraction

**Supplementary Table 1.** Single crystal X-ray diffraction data and refinement parameters for **0%** at 295 K, 230 K and 170 K measured on the same crystal.

	295 K	230 K	170 K
Empirical formula	C <sub>12</sub> H <sub>16</sub> l <sub>2</sub> N <sub>4</sub> OSm	C <sub>12</sub> H <sub>16</sub> l <sub>2</sub> N <sub>4</sub> OSm	C <sub>12</sub> H <sub>16</sub> l <sub>2</sub> N <sub>4</sub> OSm
Formula weight	636.44	636.44	636.44
Temperature/K	295.00	230.00	169.99
Crystal system	Monoclinic	Monoclinic	Monoclinic
Space group	<i>P2<sub>1</sub>/m</i>	<i>P2<sub>1</sub>/m</i>	<i>P2<sub>1</sub>/m</i>
<i>a</i> /Å	9.07712(19)	9.0249(3)	8.94497(13)
<i>b</i> /Å	8.15614(16)	8.0968(3)	7.93580(13)
<i>c</i> /Å	12.7219(3)	12.6429(4)	12.43051(18)
<i>α</i> /°	90	90	90
<i>β</i> /°	94.6744(19)	94.567(3)	93.4456(15)
<i>γ</i> /°	90	90	90
Volume/Å <sup>3</sup>	938.73(3)	920.92	880.79(2)
<i>Z</i>	2	2	2
$\rho_{\text{calc}}$ / g/cm <sup>3</sup>	2.252	2.295	2.400
$\mu$ /mm <sup>-1</sup>	49.319	50.273	52.563
<i>F</i> (000)	584.0	584.0	584.0
Crystal size/mm <sup>3</sup>	0.112 x 0.036 x 0.029	0.11 x 0.049 x 0.035	0.108 x 0.039 x 0.027
Radiation	Cu K $\alpha$ ( $\lambda$ = 1.54184)	Cu K $\alpha$ ( $\lambda$ = 1.54184)	Cu K $\alpha$ ( $\lambda$ = 1.54184)
2 $\theta$ range /°	6.972 to 153.496	7.014 to 153.95	7.124 to 152.836
Index ranges	-11 ≤ <i>h</i> ≤ 11, -10 ≤ <i>k</i> ≤ 10, -15 ≤ <i>l</i> ≤ 15	-8 ≤ <i>h</i> ≤ 11, -10 ≤ <i>k</i> ≤ 10, -15 ≤ <i>l</i> ≤ 15	-8 ≤ <i>h</i> ≤ 11, -9 ≤ <i>k</i> ≤ 9, -15 ≤ <i>l</i> ≤ 15
Reflections collected	19406	19277	18187
Independent reflections	2109 [ <i>R</i> <sub>int</sub> = 0.0789, <i>R</i> <sub>sigma</sub> = 0.0338]	2080 [ <i>R</i> <sub>int</sub> = 0.0839, <i>R</i> <sub>sigma</sub> = 0.0345]	1974 [ <i>R</i> <sub>int</sub> = 0.0679, <i>R</i> <sub>sigma</sub> = 0.0273]
Data/restraints/parameters	2109 / 18 / 115	2080 / 60 / 115	1974 / 60 / 115
Goodness-of-fit on <i>F</i> <sup>2</sup>	1.040	1.044	1.041
Final <i>R</i> indexes [ <i>I</i> ≥ 2 $\sigma$ ( <i>I</i> )]	<i>R</i> <sub>1</sub> = 0.0354, <i>wR</i> <sub>2</sub> = 0.0944	<i>R</i> <sub>1</sub> = 0.0499, <i>wR</i> <sub>2</sub> = 0.1382	<i>R</i> <sub>1</sub> = 0.0504, <i>wR</i> <sub>2</sub> = 0.1331
Final <i>R</i> indexes [all data]	<i>R</i> <sub>1</sub> = 0.0403, <i>wR</i> <sub>2</sub> = 0.1019	<i>R</i> <sub>1</sub> = 0.0567, <i>wR</i> <sub>2</sub> = 0.1494	<i>R</i> <sub>1</sub> = 0.0550, <i>wR</i> <sub>2</sub> = 0.1400
Largest diff. peak/hole / e Å <sup>-3</sup>	0.95 / -0.99	2.76 / -1.65	3.11 / -1.08

**Supplementary Table 2.** Single crystal X-ray diffraction data and refinement parameters for **Ca-100%** and **Sr-100%** at 295 K.

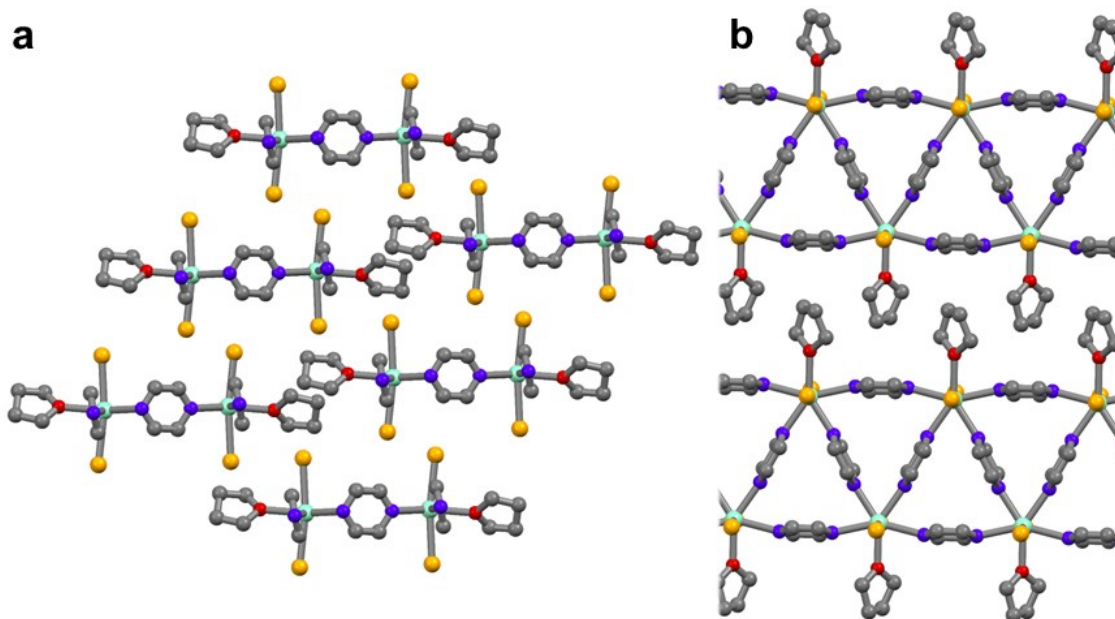
	<b>Sr-100%</b>	<b>Ca-100%</b>
Empirical formula	C <sub>12</sub> H <sub>16</sub> l <sub>2</sub> N <sub>4</sub> OSr	C <sub>12</sub> H <sub>16</sub> l <sub>2</sub> N <sub>4</sub> Oca
Formula weight	573.71	526.17
Temperature/K	294.99	294.99
Crystal system	Monoclinic	Monoclinic
Space group	<i>P2<sub>1</sub>/m</i>	<i>P2<sub>1</sub>/m</i>
<i>a</i> /Å	9.07390(10)	8.97390(10)
<i>b</i> /Å	8.20390(10)	7.98790(10)
<i>c</i> /Å	12.71610(10)	12.6087(2)
$\alpha$ /°	90	90
$\beta$ /°	94.7400(10)	94.220(2)
$\gamma$ /°	90	90
Volume/Å <sup>3</sup>	943.366(17)	901.37(2)
<i>Z</i>	2	2
$\rho_{\text{calc}}$ / g/cm <sup>3</sup>	2.020	1.939
$\mu$ /mm <sup>-1</sup>	29.678	29.907
<i>F</i> (000)	536.0	500.0
Crystal size/mm <sup>3</sup>	0.473 x 0.112 x 0.09	0.042 x 0.029 x 0.018
Radiation	Cu K $\alpha$ ( $\lambda$ = 1.54184)	Cu K $\alpha$ ( $\lambda$ = 1.54184)
2 $\theta$ range /°	6.976 to 152.924	7.03 to 153.22
Index ranges	-8 ≤ <i>h</i> ≤ 11, -9 ≤ <i>k</i> ≤ 10, -15 ≤ <i>l</i> ≤ 16	-11 ≤ <i>h</i> ≤ 11, -9 ≤ <i>k</i> ≤ 7, -15 ≤ <i>l</i> ≤ 15
Reflections collected	9871	10363
Independent reflections	2106 [ <i>R</i> <sub>int</sub> = 0.0408, <i>R</i> <sub>sigma</sub> = 0.0210]	2021 [ <i>R</i> <sub>int</sub> = 0.0421, <i>R</i> <sub>sigma</sub> = 0.0298]
Data/restraints/parameters	2106 / 30 / 116	2021 / 60 / 115
Goodness-of-fit on <i>F</i> <sup>2</sup>	1.087	1.034
Final <i>R</i> indexes [ <i>I</i> ≥ 2 $\sigma$ ( <i>I</i> )]	<i>R</i> <sub>1</sub> = 0.0364, <i>wR</i> <sub>2</sub> = 0.1039	<i>R</i> <sub>1</sub> = 0.0276, <i>wR</i> <sub>2</sub> = 0.0658
Final <i>R</i> indexes [all data]	<i>R</i> <sub>1</sub> = 0.0365, <i>wR</i> <sub>2</sub> = 0.1042	<i>R</i> <sub>1</sub> = 0.0333, <i>wR</i> <sub>2</sub> = 0.0697
Largest diff. peak/hole / e Å <sup>-3</sup>	1.49 / -1.35	1.74 / -0.57

**Supplementary Table 3.** Average M–ligand bond lengths (X = Br, I; M = Ca, Sr, Sm, Yb).

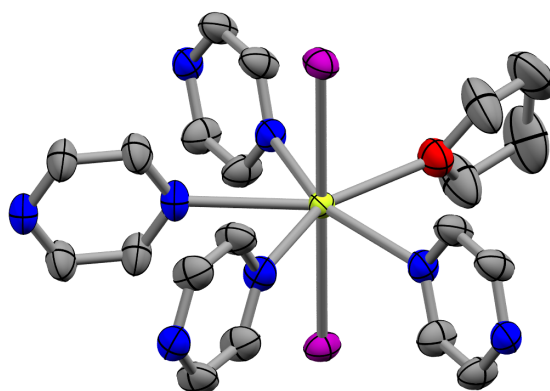
Compound	Oxidation state	M–N <sub>av</sub> (Å)	M–X <sub>av</sub> (Å)	T (K)
LT–0%	+3	2.55(1)	3.09(2)	170
RT–100%*	+3	2.52(1)	2.97(1)	295
RT–0%	+2	2.75(1)	3.19(1)	295
Sr–100%	+2	2.77(1)	3.21(1)	295
Ca–100%	+2	2.66(1)	3.09(1)	295
Yb–100%**	+2	2.63(2)	3.09(1)	230

\*Structural model based on Rietveld refinement

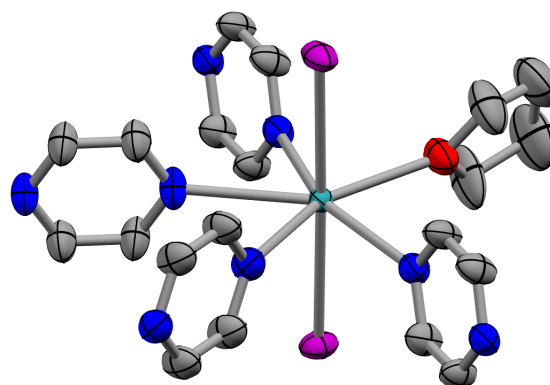
\*\*In YbI<sub>2</sub>(pyz)<sub>3</sub> at 230 K<sup>1</sup>



**Supplementary Fig. 1.** Structural model of **100%** based on Rietveld refinement. a, View along the “ribbons”, showing a slightly staggered packing. b, View perpendicular to the ribbon-plane shows interdigitation between the pendant thf ligands. Color code: Sm (teal), Br (yellow), O (red), N (blue), C (grey). H atoms omitted for clarity. Only one of the disordered positions of the thf is shown.



**Supplementary Fig. 2.** Coordination sphere of **Ca-100%** determined by SCXRD at 295 K. Thermal ellipsoids shown at 50% probability level. Color code: Ca (yellow), I (purple), O (red), N (blue), C (grey). Hydrogen atoms omitted for clarity. Selected bond lengths (Å): Ca—I 3.0920(9), 3.0878(9); Ca—N<sub>av</sub> 2.662(3).



**Supplementary Fig. 3.** Coordination sphere of **Sr-100%** determined by SCXRD at 295 K. Thermal ellipsoids shown at 50% probability level. Color code: Sr (teal), I (purple), O (red), N (blue), C (grey). Hydrogen atoms omitted for clarity. Selected bond lengths (Å): Sr—I 3.2083(4), 3.2107(5); Sr—N<sub>av</sub> 2.773(3).

**Supplementary Table 4.** Unit cell and Rietveld refinement parameters for  $\text{SmI}_2(\text{pyz})_2(\text{thf})$  and solid solutions at room temperature. The agreement factors,  $R_{\text{wp}}$ , are defined by

$R_{\text{wp}} = \sqrt{\sum w_i (y_{i,\text{obs}} - y_{i,\text{calc}})^2 / \sum w_i y_{i,\text{obs}}^2} \times 100\%$ , where  $y_{i,\text{calc}}$  is the net calculated intensity,  $y_{i,\text{obs}}$  is observed intensity, and the weight factor,  $w_i$ , is  $1/\text{ESD}^2$

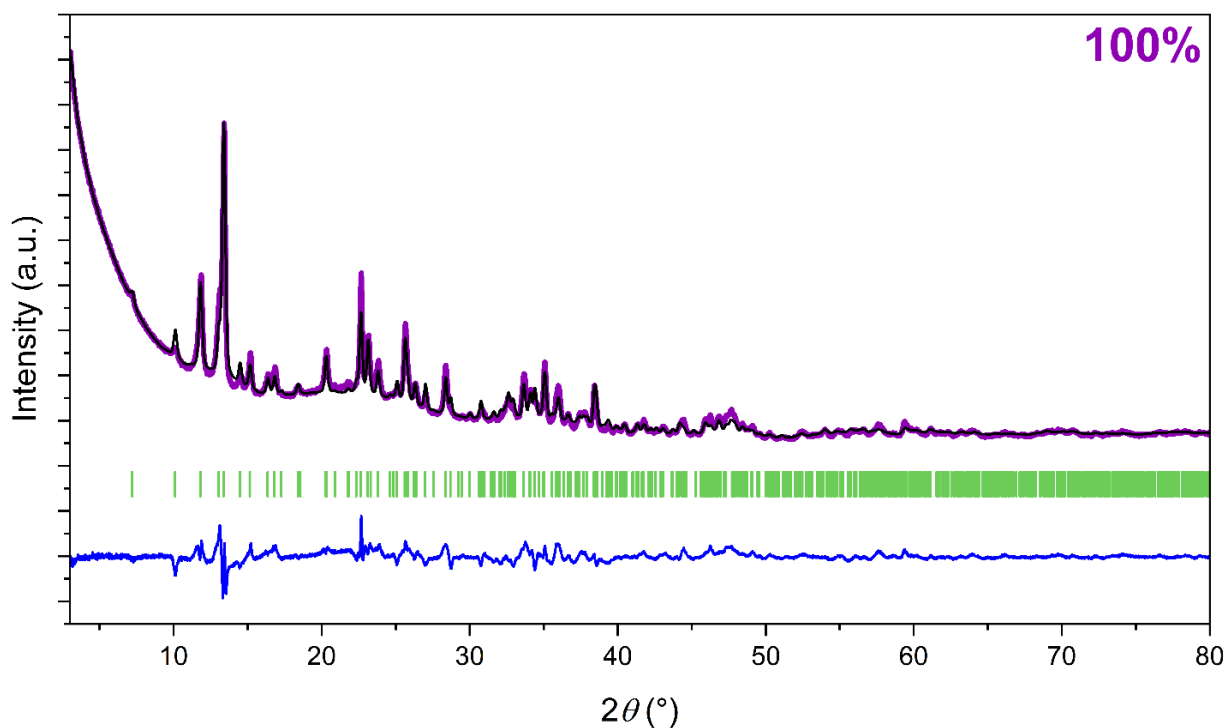
Compound	Unit cell parameters		$R_{\text{wp}}$ (%)
<b>0%</b>	$a = 9.087(1) \text{ \AA}$ $b = 8.172(1) \text{ \AA}$ $c = 12.744(1) \text{ \AA}$	$V = 943.0(1) \text{ \AA}^3$ $\alpha = \gamma = 90^\circ$ $\beta = 94.777(1)^\circ$	7.60
<b>10%</b>	$a = 9.062(1) \text{ \AA}$ $b = 8.133(2) \text{ \AA}$ $c = 12.727(3) \text{ \AA}$	$V = 934.7(2) \text{ \AA}^3$ $\alpha = \gamma = 90^\circ$ $\beta = 94.808(8)^\circ$	7.59
<b>20%</b>	$a = 9.057(1) \text{ \AA}$ $b = 8.121(1) \text{ \AA}$ $c = 12.718(1) \text{ \AA}$	$V = 932.1(1) \text{ \AA}^3$ $\alpha = \gamma = 90^\circ$ $\beta = 94.837(1)^\circ$	5.68
<b>100%</b>	$a = 8.765(2) \text{ \AA}$ $b = 7.848(2) \text{ \AA}$ $c = 12.274(2) \text{ \AA}$	$V = 839.7(3) \text{ \AA}^3$ $\alpha = \gamma = 90^\circ$ $\beta = 95.976(6)^\circ$	6.19

**Supplementary Table 5.** Unit cell and Rietveld refinement parameters for solid solutions of  $\text{SrI}_2$  in  $\text{SmI}_2(\text{pyz})_2(\text{thf})$  at room temperature.

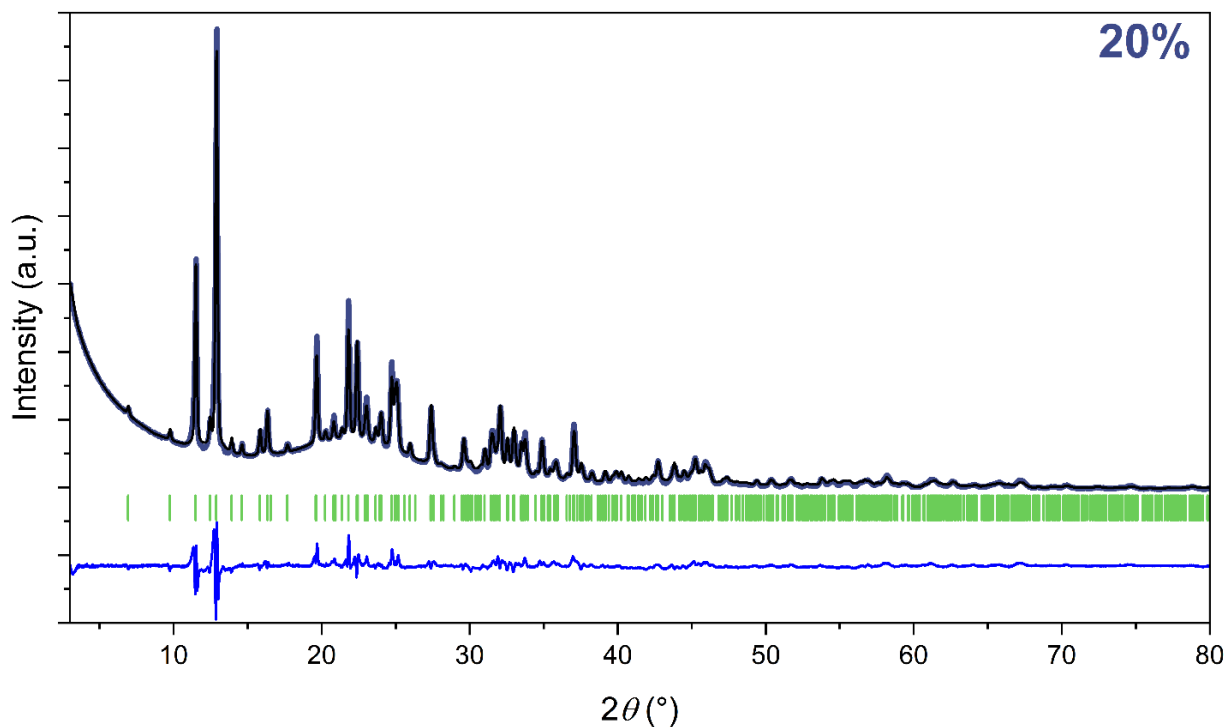
Compound	Unit cell parameters		$R_{\text{wp}}$ (%)
<b>Sr-7.5%</b>	$a = 9.076(3) \text{ \AA}$ $b = 8.160(2) \text{ \AA}$ $c = 12.730(4) \text{ \AA}$	$V = 942.5(2) \text{ \AA}^3$ $\alpha = \gamma = 90^\circ$ $\beta = 94.770(1)^\circ$	7.81
<b>Sr-15%</b>	$a = 9.072(3) \text{ \AA}$ $b = 8.157(3) \text{ \AA}$ $c = 12.726(4) \text{ \AA}$	$V = 938.5(2) \text{ \AA}^3$ $\alpha = \gamma = 90^\circ$ $\beta = 94.782(1)^\circ$	6.99

**Supplementary Table 6.** Unit cell and Rietveld refinement parameters for solid solutions of  $\text{CaI}_2$  in  $\text{SmI}_2(\text{pyz})_2(\text{thf})$  at room temperature.

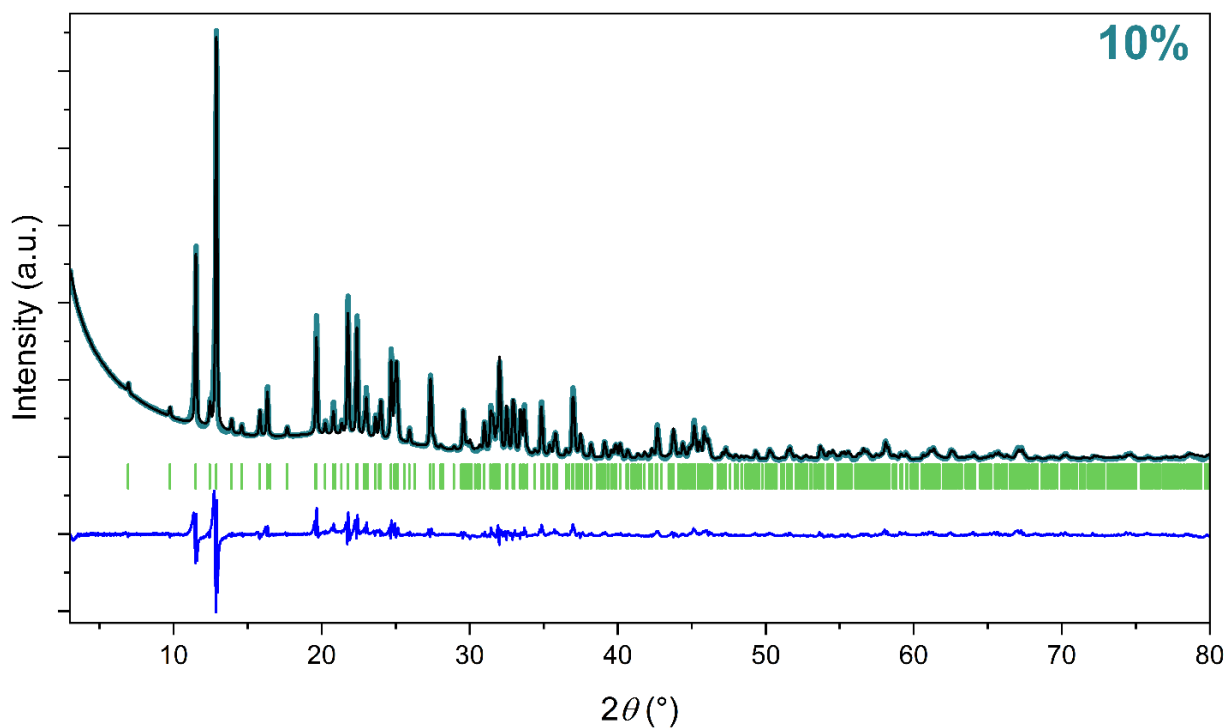
Compound	Unit cell parameters		$R_{\text{wp}}$ (%)
<b>Ca-10%</b>	$a = 9.065(4) \text{ \AA}$ $b = 8.134(3) \text{ \AA}$ $c = 12.729(5) \text{ \AA}$	$V = 935.4(2) \text{ \AA}^3$ $\alpha = \gamma = 90^\circ$ $\beta = 94.691(1)^\circ$	5.69
<b>Ca-20%</b>	$a = 9.049(1) \text{ \AA}$ $b = 8.128(1) \text{ \AA}$ $c = 12.688(1) \text{ \AA}$	$V = 930.1(1) \text{ \AA}^3$ $\alpha = \gamma = 90^\circ$ $\beta = 94.693(1)^\circ$	6.55



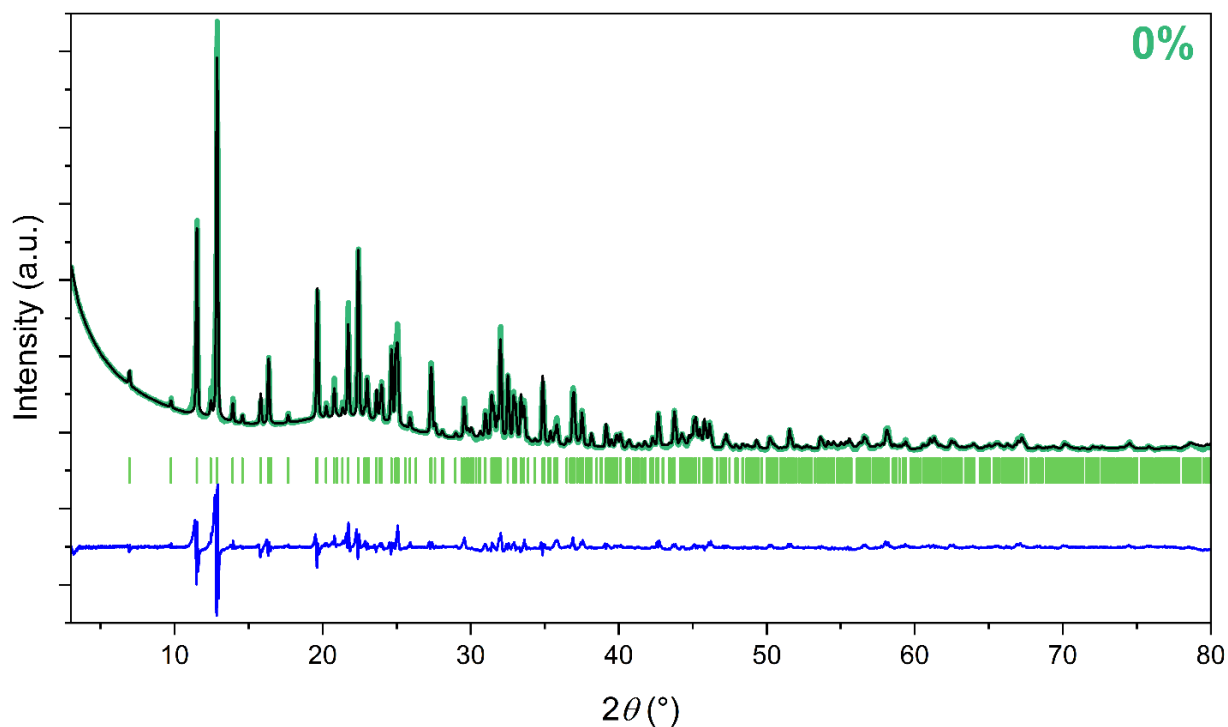
**Supplementary Fig. 4.** Room-temperature powder X-ray diffractogram of **100%** (purple) together with the Rietveld refinement (black), residual (blue), and symmetry-allowed peak positions (green).



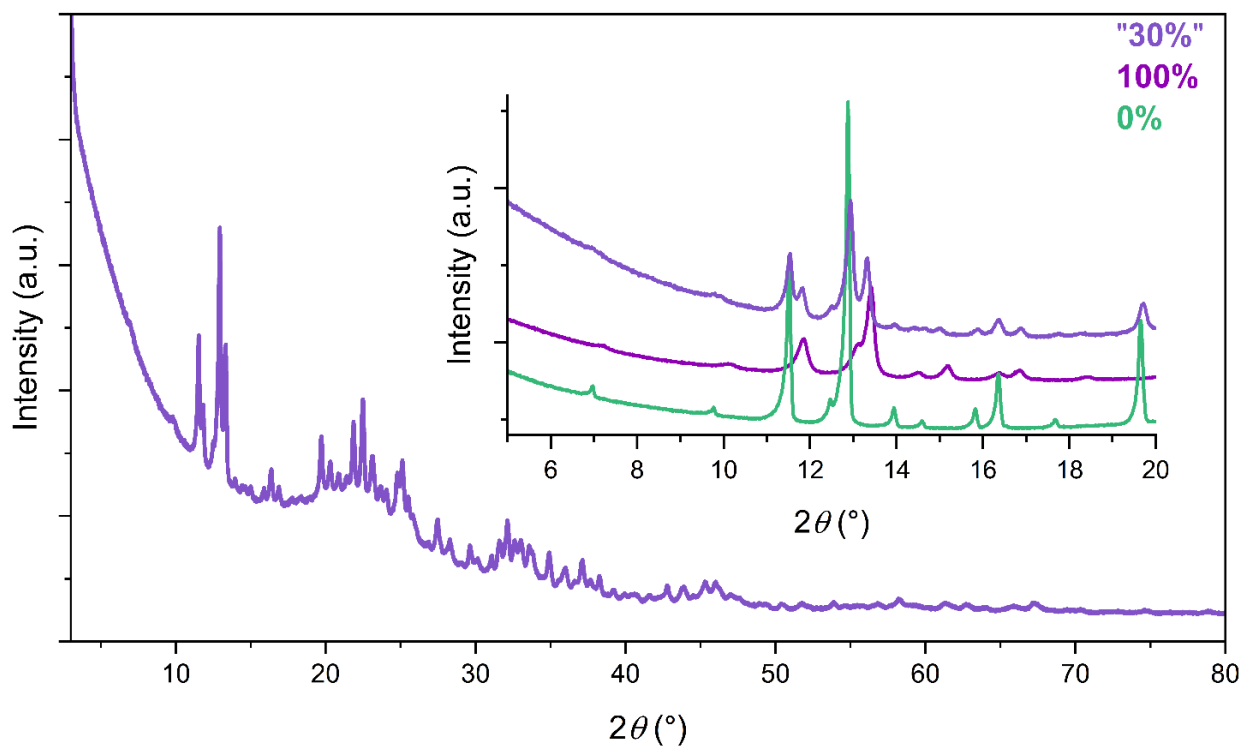
**Supplementary Fig. 5.** Room-temperature powder X-ray diffractogram of **20%** (blue) together with the Rietveld refinement (black), residual (blue), and symmetry-allowed peak positions (green).



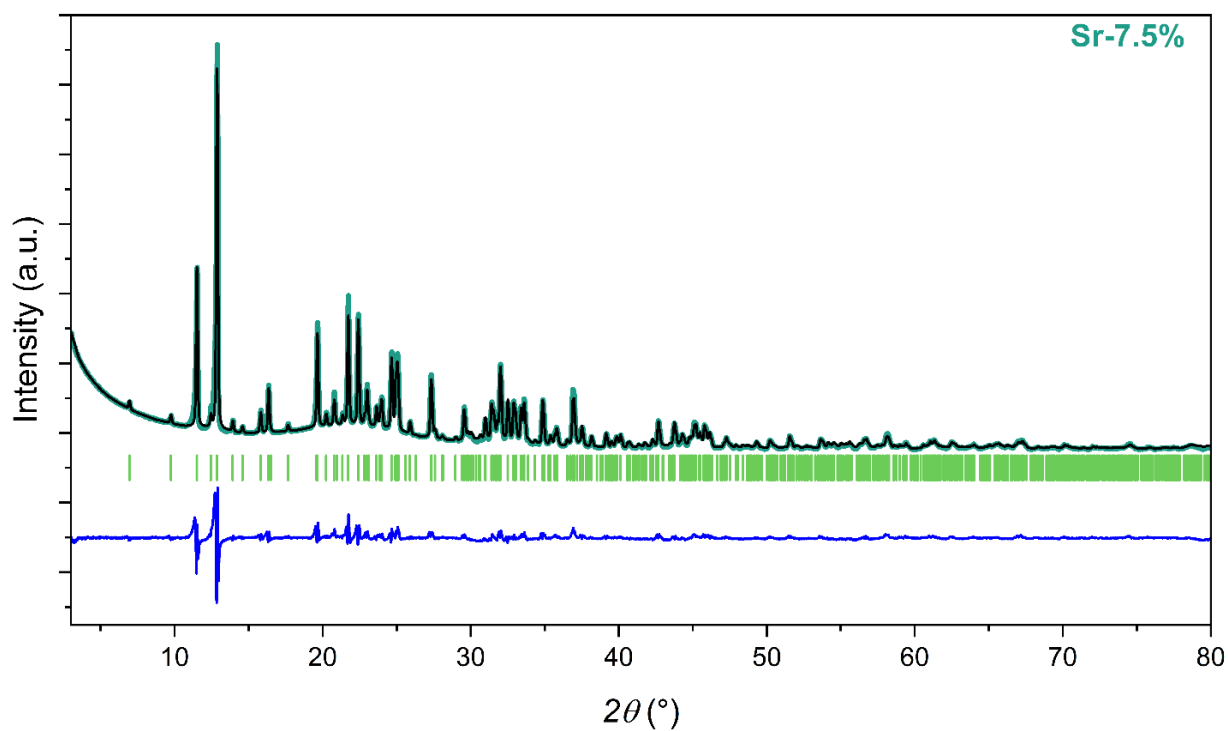
**Supplementary Fig. 6.** Room-temperature powder X-ray diffractogram of **10%** (turquoise) together with the Rietveld refinement (black), residual (blue), and symmetry-allowed peak positions (green).



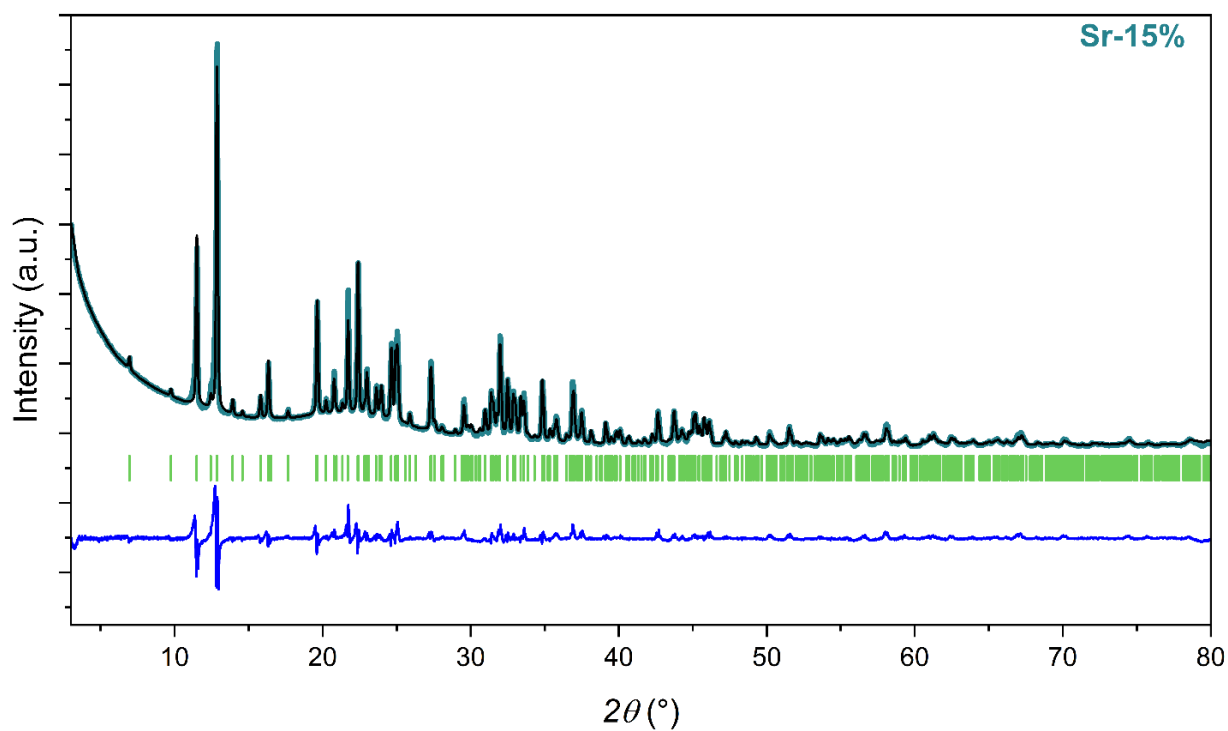
**Supplementary Fig. 7.** Room-temperature powder X-ray diffractogram of **0%** (light green) together with the Rietveld refinement (black), residual (blue), and symmetry-allowed peak positions (green).



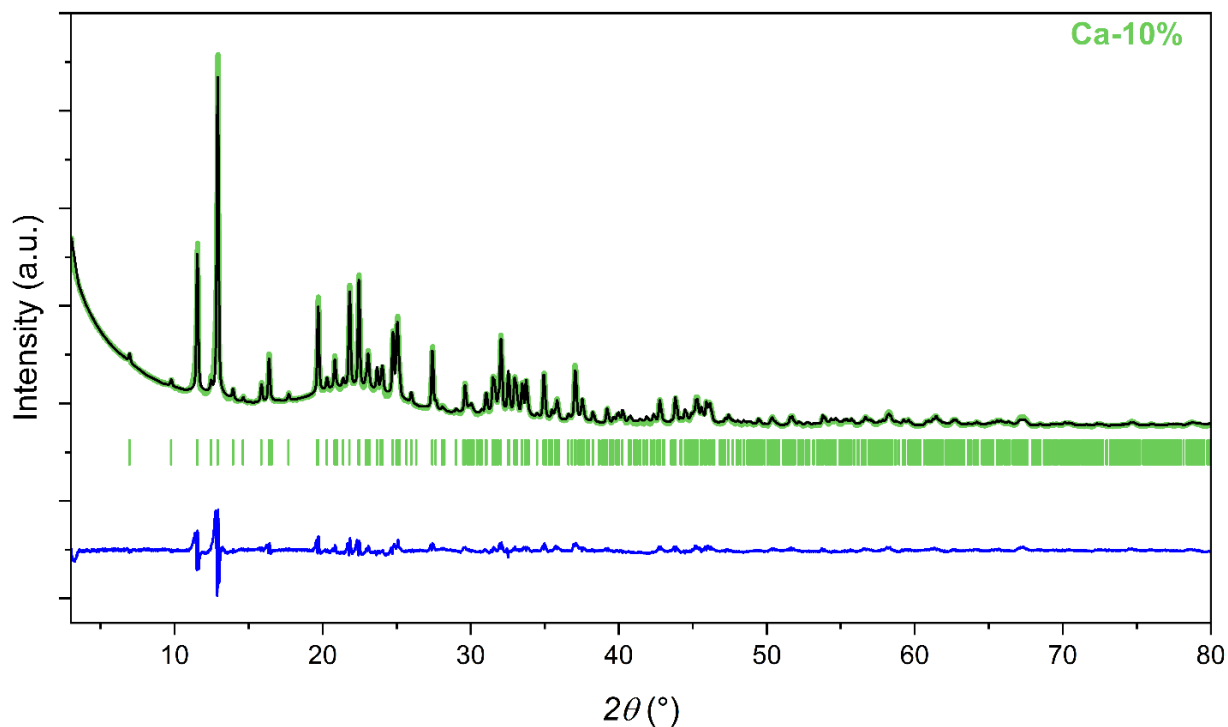
**Supplementary Fig. 8.** Room-temperature powder X-ray diffractogram of **"30%"** (lilac). The inset shows the range 3-20° with **0%** and **100%** overlaid. A mixture of the two phases is observed.



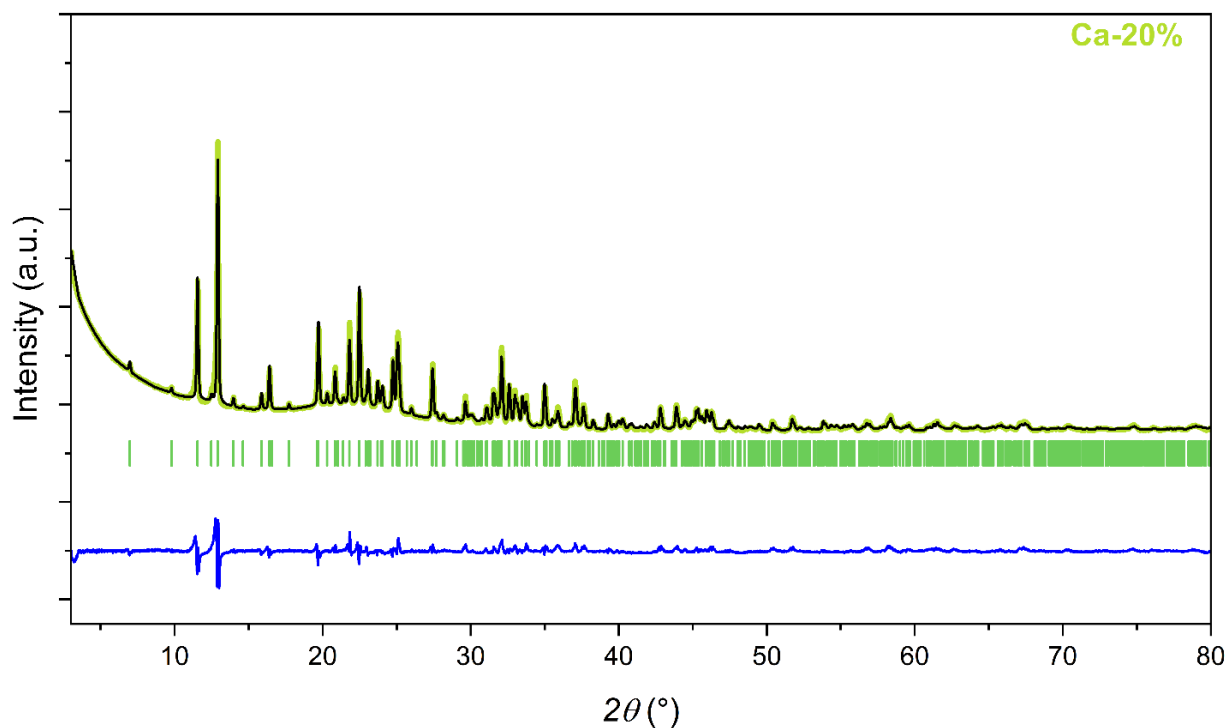
**Supplementary Fig. 9.** Room-temperature PXRD of **Sr-7.5%** (turquoise) together with the Rietveld refinement (black), residual (blue), and symmetry-allowed peak positions (green).



**Supplementary Fig. 10.** Room-temperature PXRD of **Sr-15%** (blue-green) together with the Rietveld refinement (black), residual (blue), and symmetry-allowed peak positions (green).

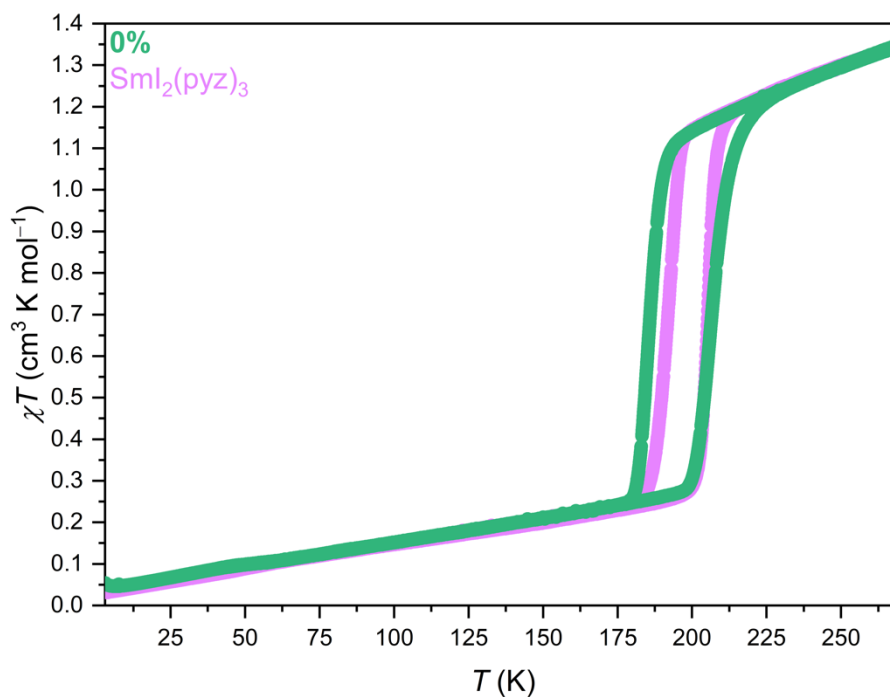


**Supplementary Fig. 11.** Room-temperature PXRD of **Ca-10%** (turquoise) together with the Rietveld refinement (black), residual (blue), and symmetry-allowed peak positions (green).

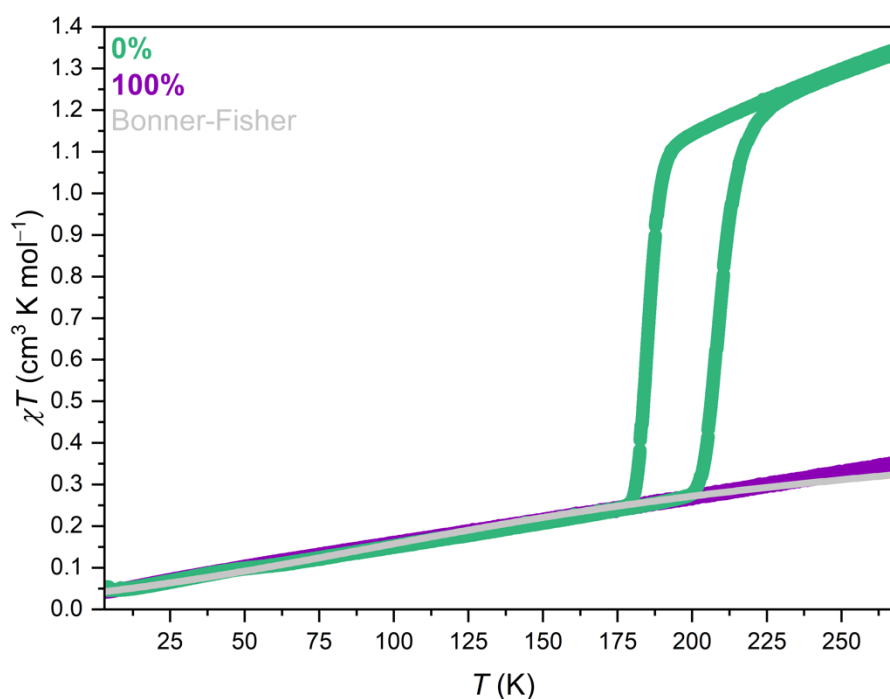


**Supplementary Fig. 12.** Room-temperature PXRD of **Ca-20%** (turquoise) together with the Rietveld refinement (black), residual (blue), and symmetry-allowed peak positions (green).

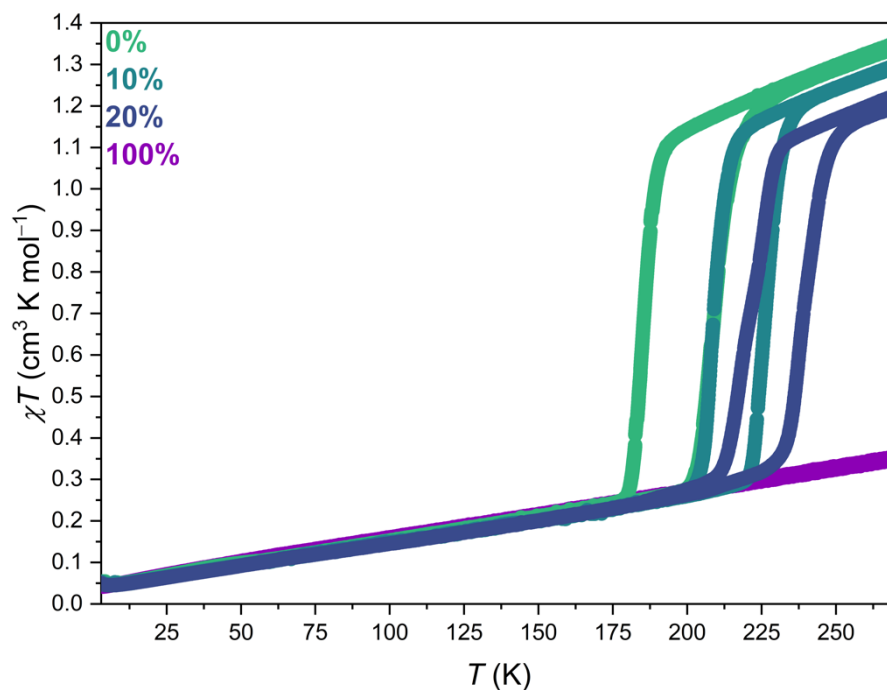
## Magnetization Data



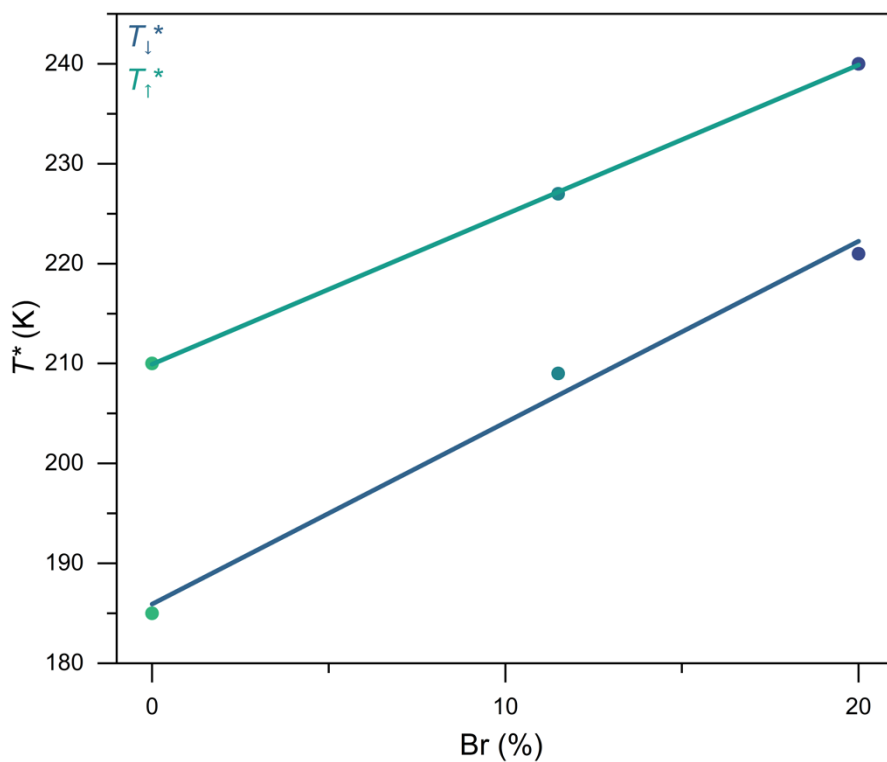
**Supplementary Fig. 13.** Temperature dependence of  $\chi T$  (3-270 K) for  $\text{Sml}_2(\text{pyZ})_3$  and 0%.



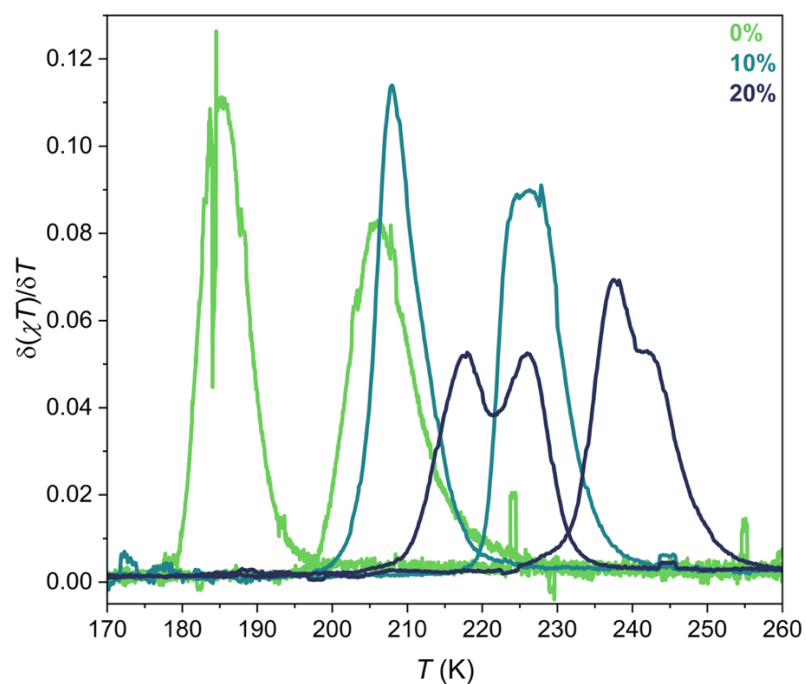
**Supplementary Fig. 14.** Temperature dependence of  $\chi T$  (3-270 K) for 0% and 100% with a Bonner-Fisher model of antiferromagnetically coupled  $S = \frac{1}{2}$  spins, with an exchange coupling constant of  $J = -75 \text{ cm}^{-1}$ , in gray.



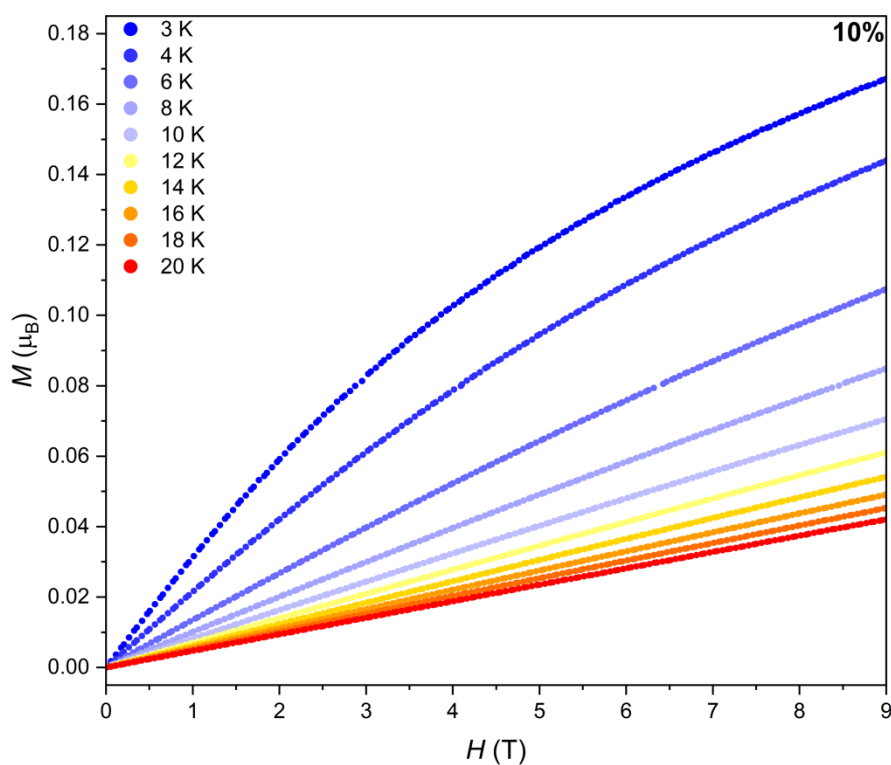
**Supplementary Fig. 15.** Temperature dependence of  $\chi T$  (3–270 K) for **0%**, **10%**, **20%** and **100%**.



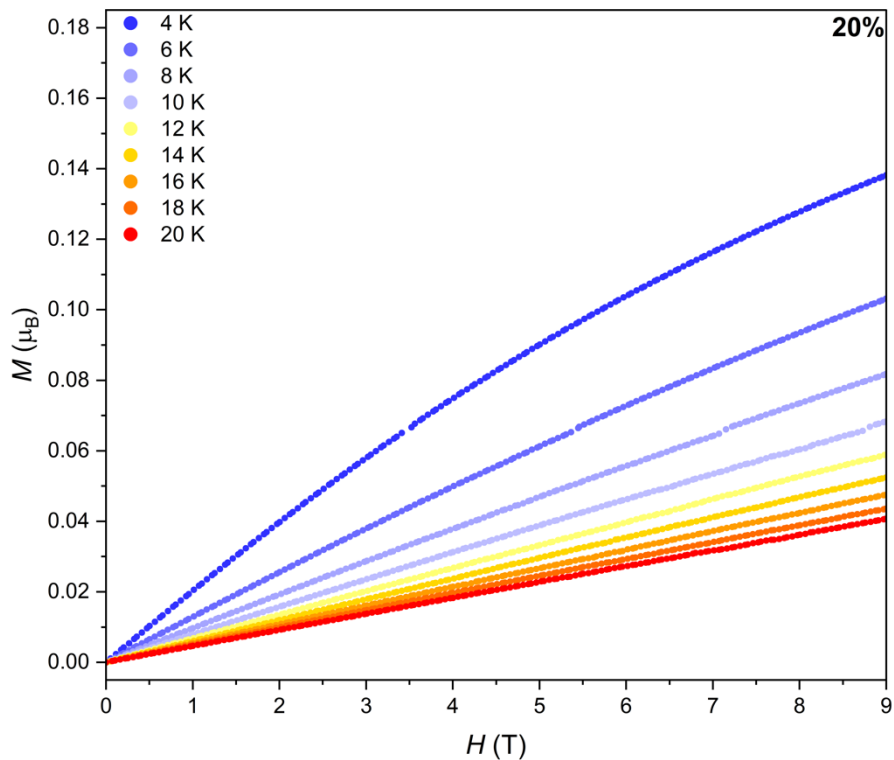
**Supplementary Fig. 16.** Transition temperature dependence on Br % (from 0 to 20%). Points are experimental data; lines are linear fits.



**Supplementary Fig. 17.** First derivative of  $\chi T$  for **0%**, **10%** and **20%** with respect to  $T$ . The derivatives have been smoothed using an adjacent-averaging function (20-point averaging).

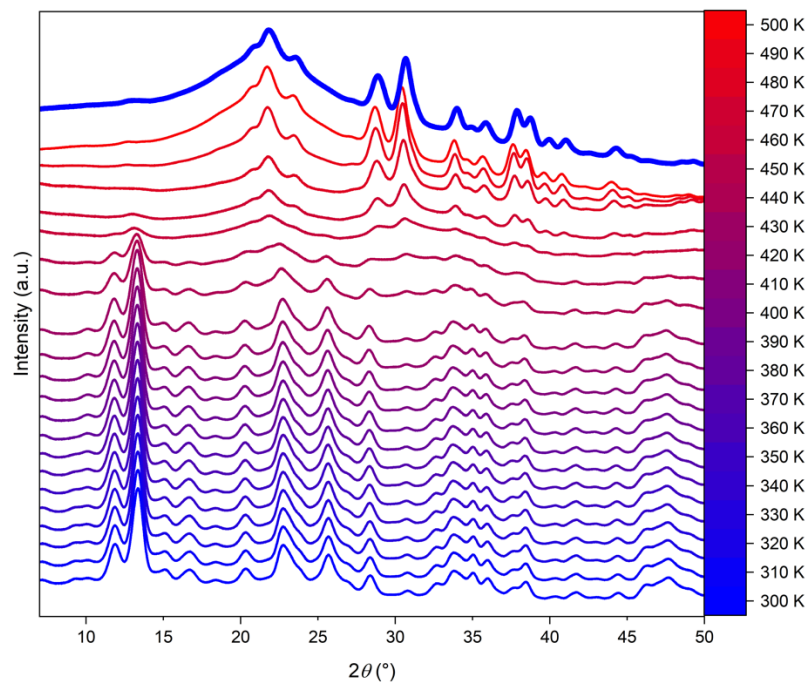


**Supplementary Fig. 18.** Magnetization of **10%** as a function of applied field from 0 to 9 T at 3 K and from 4–20 K in steps of 2 K.



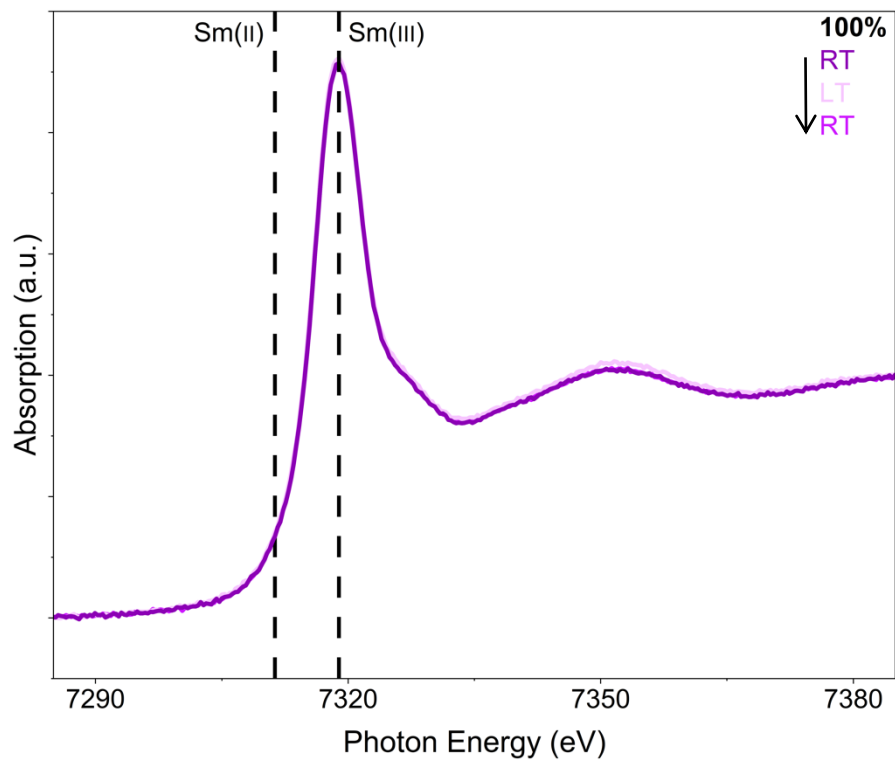
**Supplementary Fig. 19.** Magnetization of 20% as a function of applied field from 0 to 9 T from 4–20 K in steps of 2 K.

**Temperature Dependence of the Powder X-ray Diffractogram of 100%**

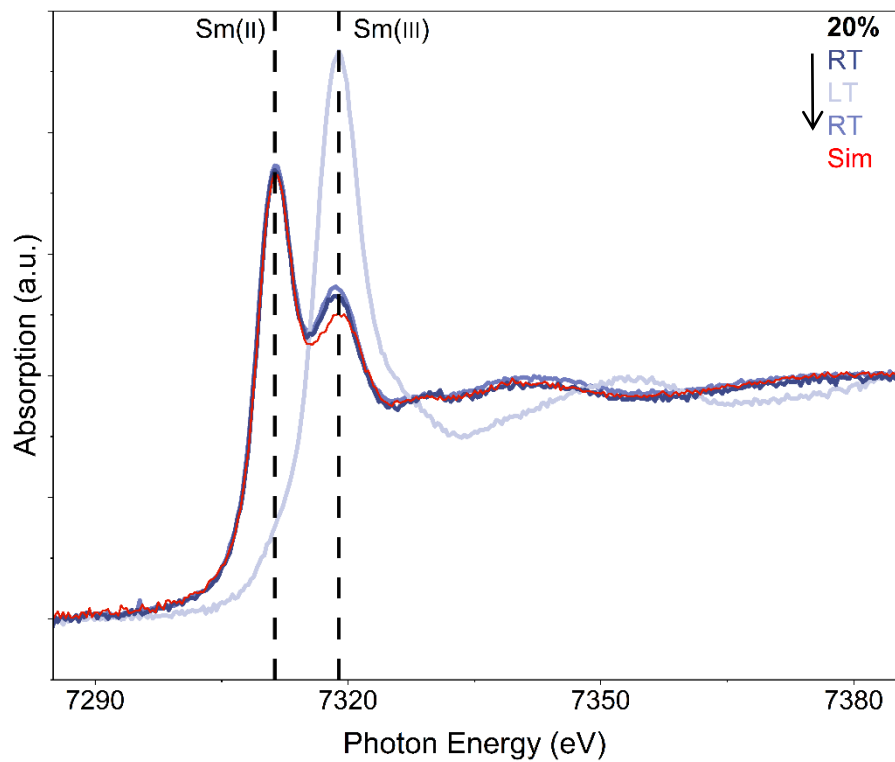


**Supplementary Fig. 20.** Temperature dependent PXRD from 300–500 K.

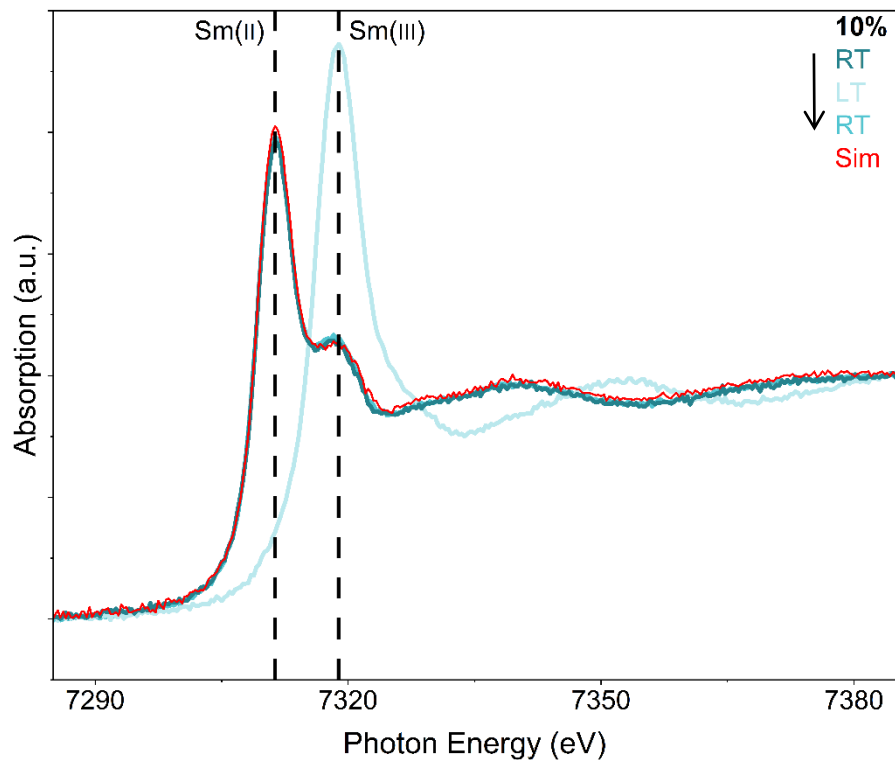
## X-Ray Absorption Spectroscopy



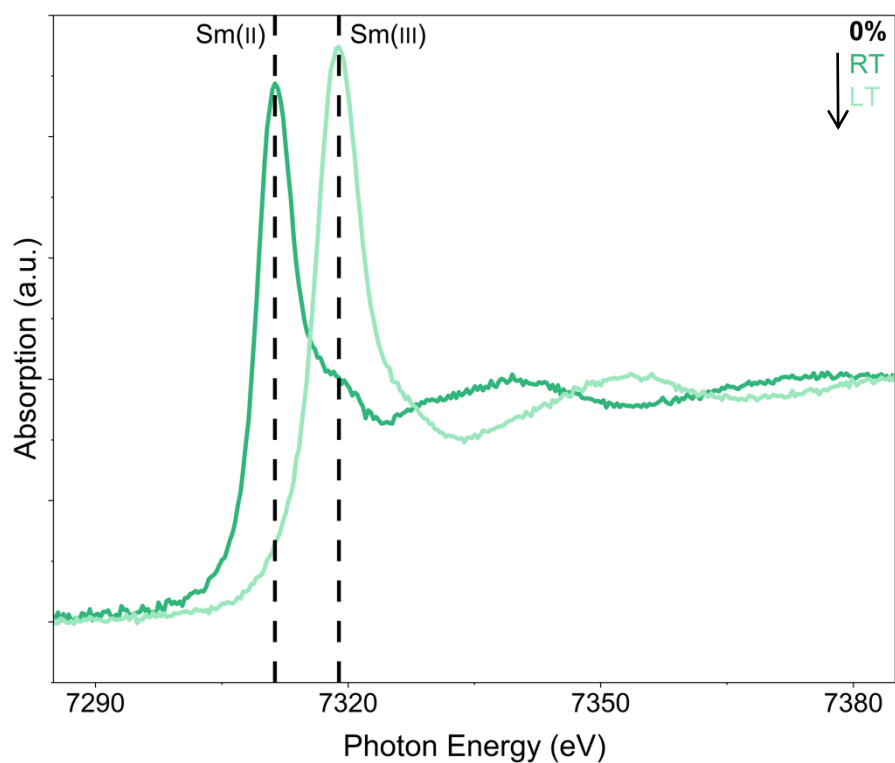
**Supplementary Fig. 21.** XANES spectra of **100%** measured at room temperature, then at ~50 K, then at room temperature again.



**Supplementary Fig. 22.** XANES spectra of **20%** measured at room temperature, then at  $\sim 50$  K, then at room temperature again. The simulation (in red) is as described in the main text with coefficients for the linear combinations: 0.8 of **0%** and 0.2 of **100%**.

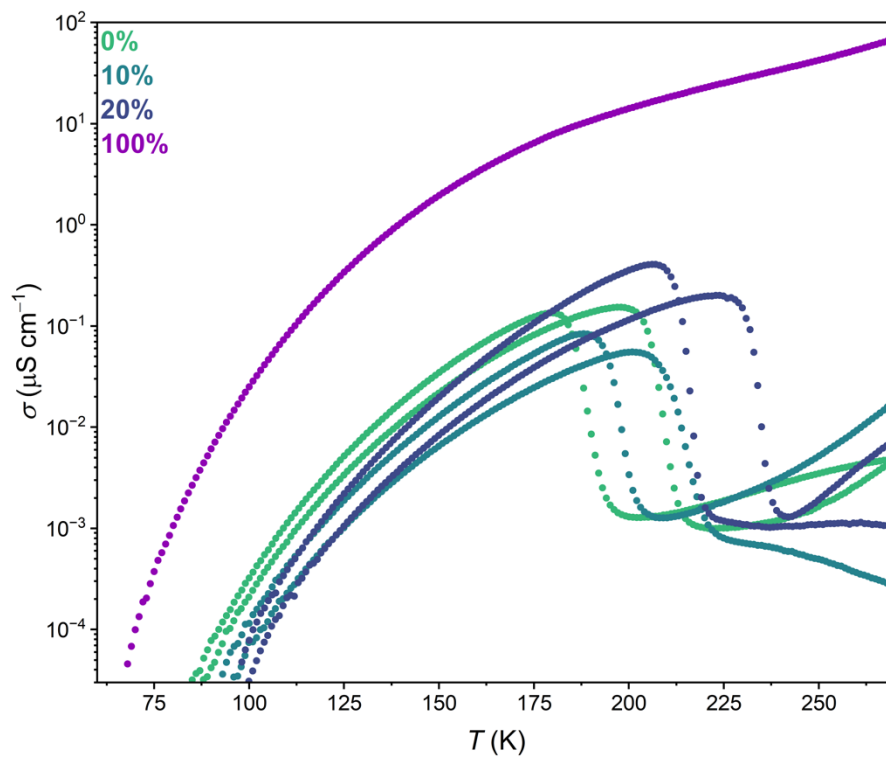


**Supplementary Fig. 23.** XANES spectra of **10%** measured at room temperature, then at  $\sim 50$  K, then at room temperature again. The simulation (in red) is as described in the main text with coefficients for the linear combinations: 0.9 of **0%** and 0.1 of **100%**.



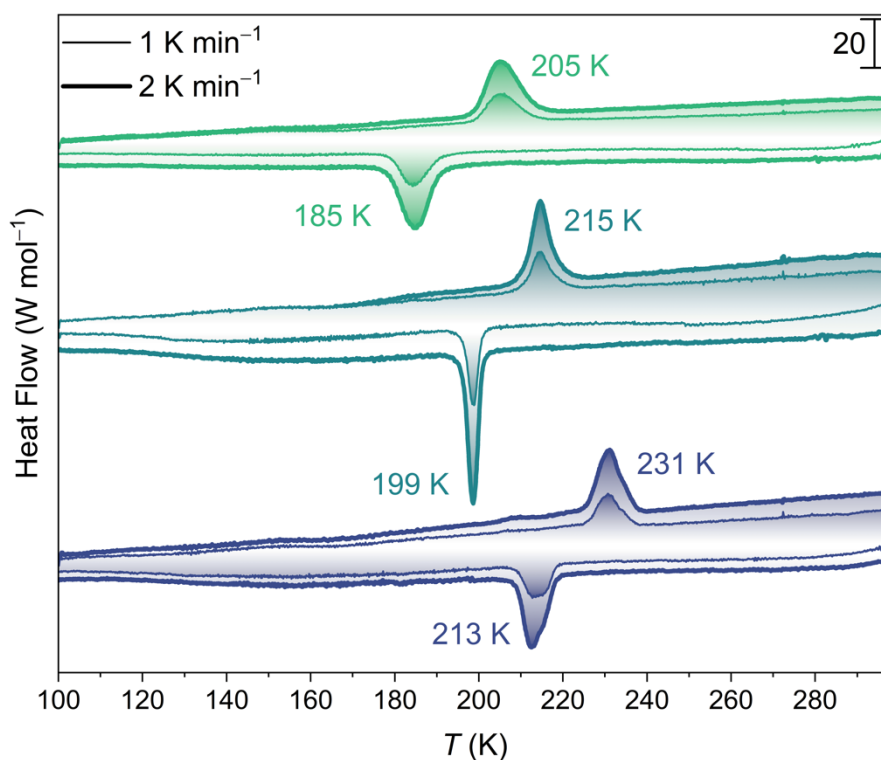
**Supplementary Fig. 24.** XANES spectra of **0%** measured at room temperature and at  $\sim 50$  K.

## Electrical Conductivity



**Supplementary Fig. 25.** Electrical conductivity of 0%, 10%, 20% and 100% measured in the range 60 K to 270 K.

## Differential Scanning Calorimetry



**Supplementary Fig. 26.** DSC scans of 0%, 10%, and 20% measured in the range 298 K to 100 K, with sweep rates of 1 and 2 K min<sup>-1</sup>. For each thermodynamic event the maximum heat flow temperature is indicated.

**Supplementary Table 6.** Changes in enthalpy and entropy as calculated from DSC (with a scan rate of 2 K min<sup>-1</sup>). The final two columns show the enthalpy and entropy normalized to the experimental content of {Sml<sub>2</sub>} nodes.

Compound / direction	Max. Heat Flow (K)	$\Delta H$ (kJ mol <sup>-1</sup> )	$\Delta S$ (J mol <sup>-1</sup> K <sup>-1</sup> )	$\Delta H_{\text{norm}}$ (kJ mol <sup>-1</sup> )	$\Delta S_{\text{norm}}$ (J mol <sup>-1</sup> K <sup>-1</sup> )
0% / cool	185	-6.41	-34.7	-6.41	-34.7
0% / heat	205	-6.42	-31.3	-6.42	-31.3
10% / cool	199	-5.80	-29.2	-6.44	-32.4
10% / heat	215	-6.01	-28.0	-6.68	-31.1
20% / cool	213	-5.23	-24.6	-6.54	-30.8
20% / heat	231	-5.17	-22.4	-6.47	-28.0

## References

- (1) Dunstan, M. A.; Manvell, A. S.; Yutronkie, N. J.; Aribot, F.; Bendix, J.; Rogalev, A.; Pedersen, K. S. Tunable valence tautomerism in lanthanide–organic alloys. *Nat. Chem.* **2024**, *16*, 735–740.
- (2) Szostak, M.; Spain, M.; Procter, D. J. Determination of the Effective Redox Potentials of  $\text{SmI}_2$ ,  $\text{SmBr}_2$ ,  $\text{SmCl}_2$ , and their Complexes with Water by Reduction of Aromatic Hydrocarbons. Reduction of Anthracene and Stilbene by Samarium(II) Iodide–Water Complex. *J. Org. Chem.* **2014**, *79*, 2522–2537.
- (3) Agilent (2014). CrysAlisPro. Agilent Technologies Ltd, Oxfordshire, England.
- (4) Sheldrick, G. M. A short history of SHELX. *Acta Crystallogr. A*, **2008**, *64*, 112–122.
- (5) Sheldrick, G. M. Crystal structure refinement with SHELXL. *Acta Crystallogr. C*, **2015**, *71*, 3–8.
- (6) Dolomanov, O.V.; Bourhis, L.J.; Gildea, R.J.; Howard, J.A.K.; Puschmann, H. OLEX2: a complete structure solution, refinement and analysis program. *J. Appl. Cryst.* **2009**, *42*, 339–341.
- (7) Degen, T.; Sadki, M.; Bron, E.; König, U.; Nénert, G. The HighScore Suite. *Powder Diffraction*, **2014**, *29*, S13–S18.